Semi Annual report on NAGW-2023

An instrument to measure the charge, and energy spectrum (20-1000 GeV/a) of the Cosmic Ray species Oxygen to Iron

For the period March 1, 1994 through September 30, 1994

Prepared by:
Cosmic Ray Laboratories,
The University of Alabama in Huntsville,
Huntsville, AL, 35899

Dr. J. C. Gregory, Principal Investigator
Dr. A. E. Smith, Co-investigator

Contents

.

.

Introduction:

BUGS-4 (Bristol University Gas Scintillator-4) made its maiden engineering flight from Fort Sumner (NM) on the 29th of September 1993. The instrument was consumed by fire after striking a power line during landing following 24 hours at float. The analysis of the telemetered data from this sophisticated instrument is a demanding task. Early analysis was compromised by electronic artifacts. Unraveling these problems has been difficult and time consuming, especially as the flight hardware was burned beyond salvage, but it is an essential preliminary to analysis. During this report period we have concentrated on a small sub-set of data (the first 30,000 events; 90 minutes at float), and developed software algorithms to correct systematic errors. Using these corrected events we have begun to develop the analysis algorithms. Although the analysis is preliminary, and restricted to the first 30,000 events, the results are encouraging, and suggest the design concepts are well matched to this application. Further work will refine the analysis, and allow quantitative evaluation of the concepts employed in BUGS-4 for applicability to future instruments. We believe this work will justify fabrication of a new instrument employing techniques deployed on BUGS-4.
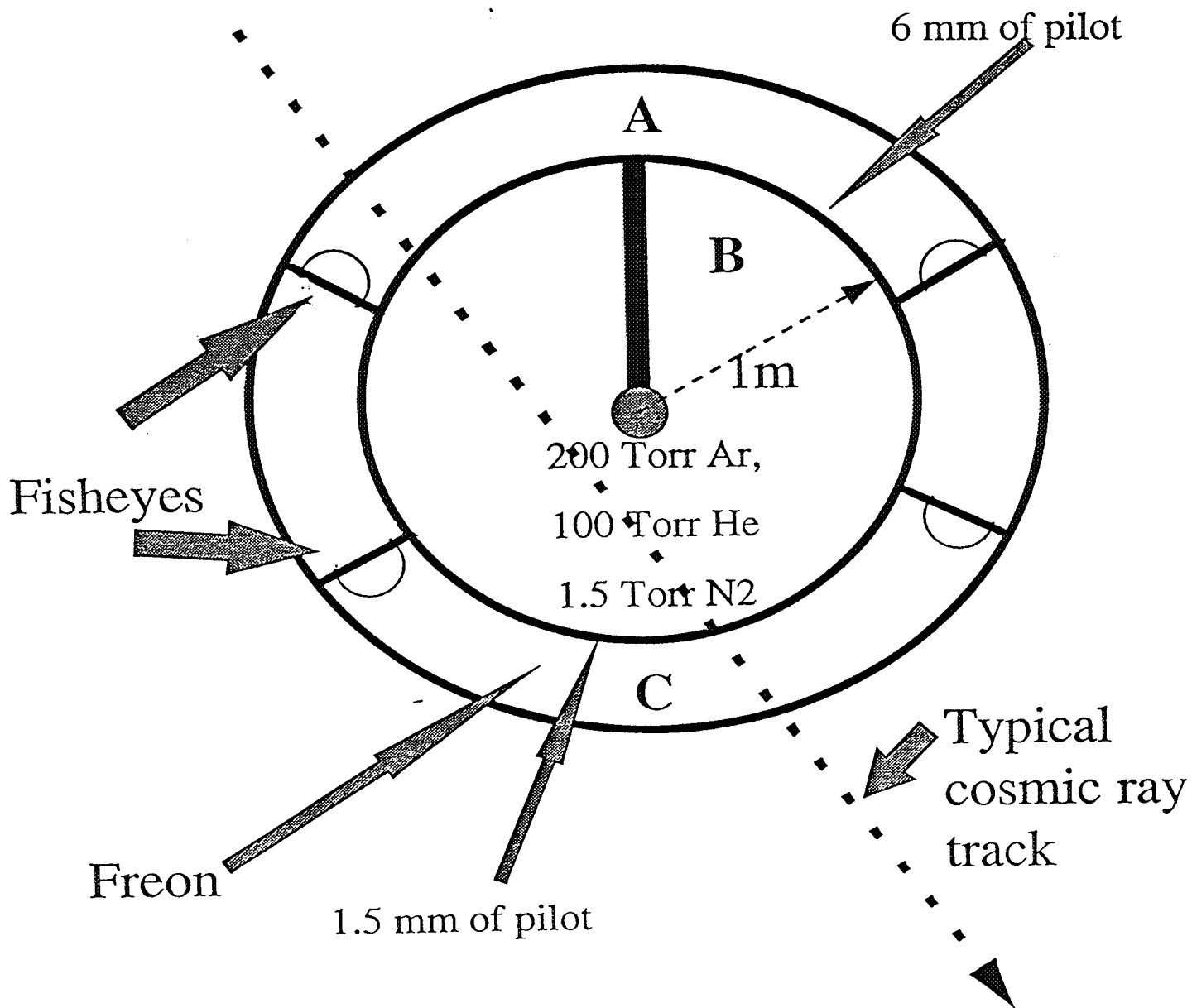
Fig 1.1 Schematic diagram of Bugs-4

1.0 Brief description of BUGS-4

1.1 Overview of operation

To aid with understanding the following sections we include a précis of the operation of BUGS-4. A schematic diagram of the instrument is shown in fig 1.1. A cosmic ray of energy < 20 GeV/a, transversing the collection aperture, experimentally determined as a coincidence between regions A and C, is measured in several ways: from region A and C a Cerenkov signal is produced from the pilot (threshold 0.4 GeV/a); from region B a primary scintillation, followed by an amplified (gain ~ 150) gas proportional signal (GPS) when the liberated electrons drift to the central electrode. The time between the primary, and GPS is proportional to the impact parameter squared: this provides a path length correction for all regions of the detector. For cosmic ray energies > 20 GeV/a a gas Cerenkov signal is produced from the freon in region C, and for energies exceeding 70 GeV/a a gas Cerenkov signal from region B.

2.0 Regions A and C

Before launch the ADC offsets were measured, and electromagnetic compatibility tests confirmed there was no interaction between the NSBF transmissions, and on-board electronics. However, the float gains and ADC offsets were different to those set before launch. Also during ballast operation there was interference between NSBF commands, and science operation. Our desire to understand the origin of these problems was frustrated by the loss of BUGS-4. However, from examining the data, as we will show, we have deduced that flight operation was constant for the first 30,000 events. Hence we have concentrated our attention on these data, and present the salient points in this report. Once the systematic errors in this sub-set have been corrected we will apply the understanding to the remaining data.

2.1 Time variation

Iron cosmic rays provide the most reliable time independent reference with which to access the time stability. In fig's 2.1(a-h) the variations in the iron centroid for each of the 8 amplified signals in region A, with a gate applied on region B, is presented. These data are grouped in 1500 event intervals with typically each 1500 events containing 450 iron nuclei. This procedure was repeated for the 8 tubes in B, and the results are shown in fig's 2.1(i-o); tube b8 failed. In the iron spectra from B there is a clear decrease in the centroid, especially for b7 (fig 2.1o), beyond 20 units (i.e., 20*1500=30,000 events), but before that the signals show no obvious trends. This behavior is also shown in the fractional yield of iron events (fig 2.1p). The increase in yield beyond 20 units, corresponds to the reduction in gain shown in figs 2.1I through 2.1o; with lower gains the efficiency for lighter elements decreases, and the fraction of iron cosmic rays increases. However, the range 1 to 20 units is, given the statistical limits, constant, and these data were used to investigate, and correct the systematic errors.

2.2 ADC offsets

To counter amplitude variations for cosmic rays at high and low latitudes, each tube signal
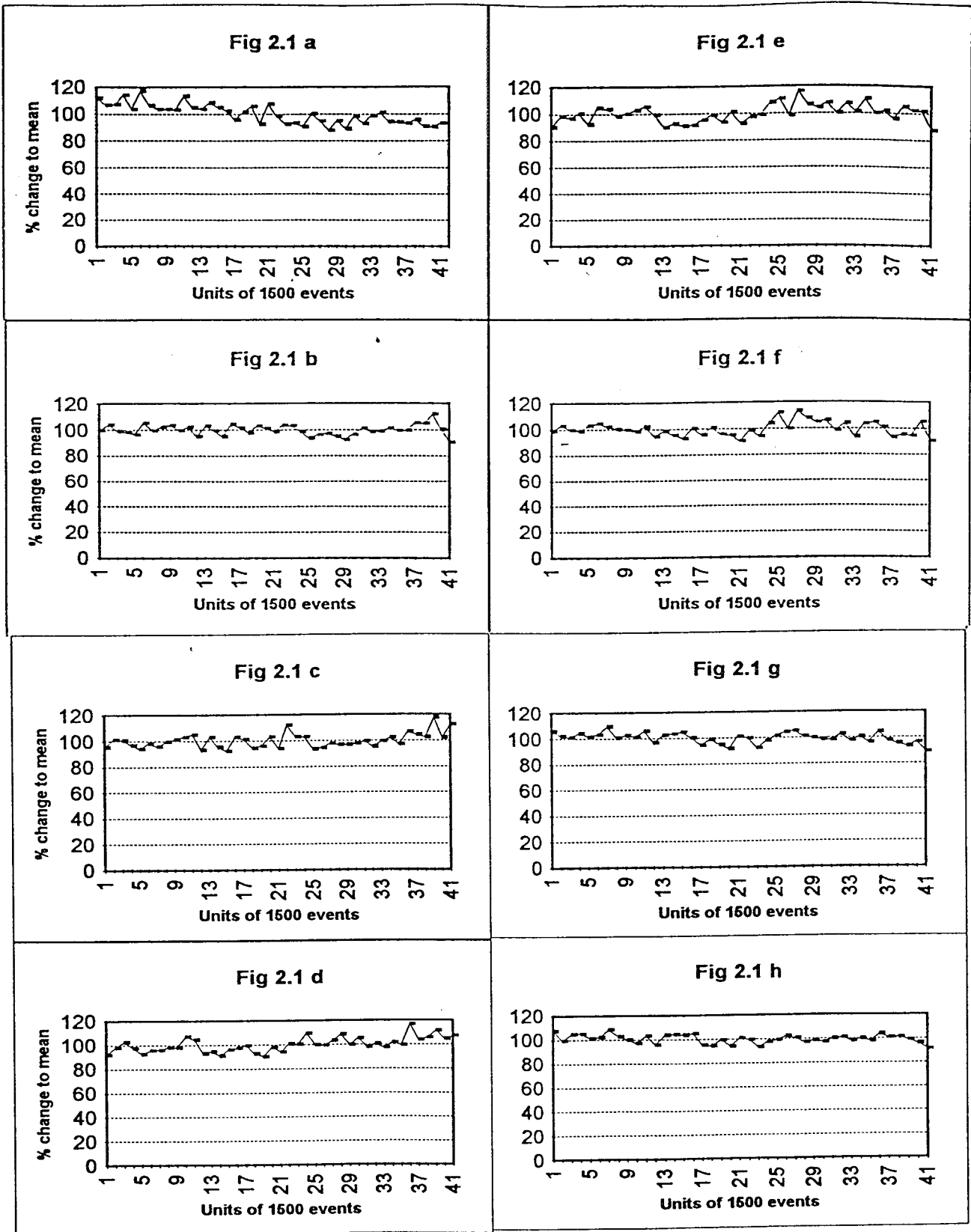
Fig 2.1 (a-h). The variation in the iron centriod for each of the eight amplified signals in region A.

Fig 2.1 i

% change to mean — Units of 1500 events

Fig 2.1 m

% change to mean — Units of 1500 events

Fig 2.1 j

% change to mean — Units of 1500 events

Fig 2.1 n

% change to mean — Units of 1500 events

Fig 2.1 k

% change to mean — Units of 1500 events

Fig 2.1 o

% change to mean — Units of 1500 events

Fig 2.1 l

% change to mean — Units of 1500 events
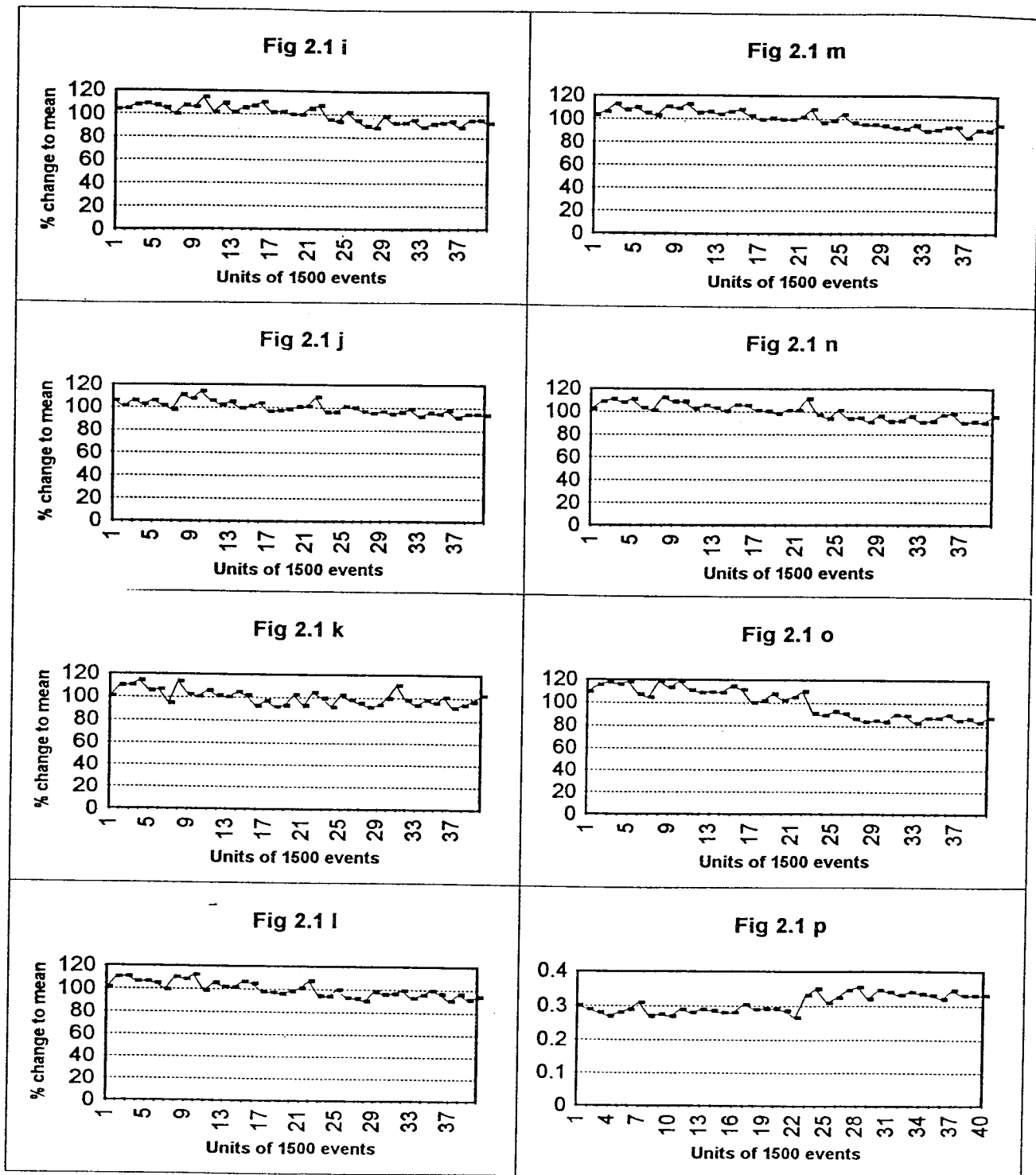
Fig 2.1 p

Units of 1500 events

Fig 2.1 (i-o) The variation in the iron centroid for tubes
in region B; Tube 8 failed.
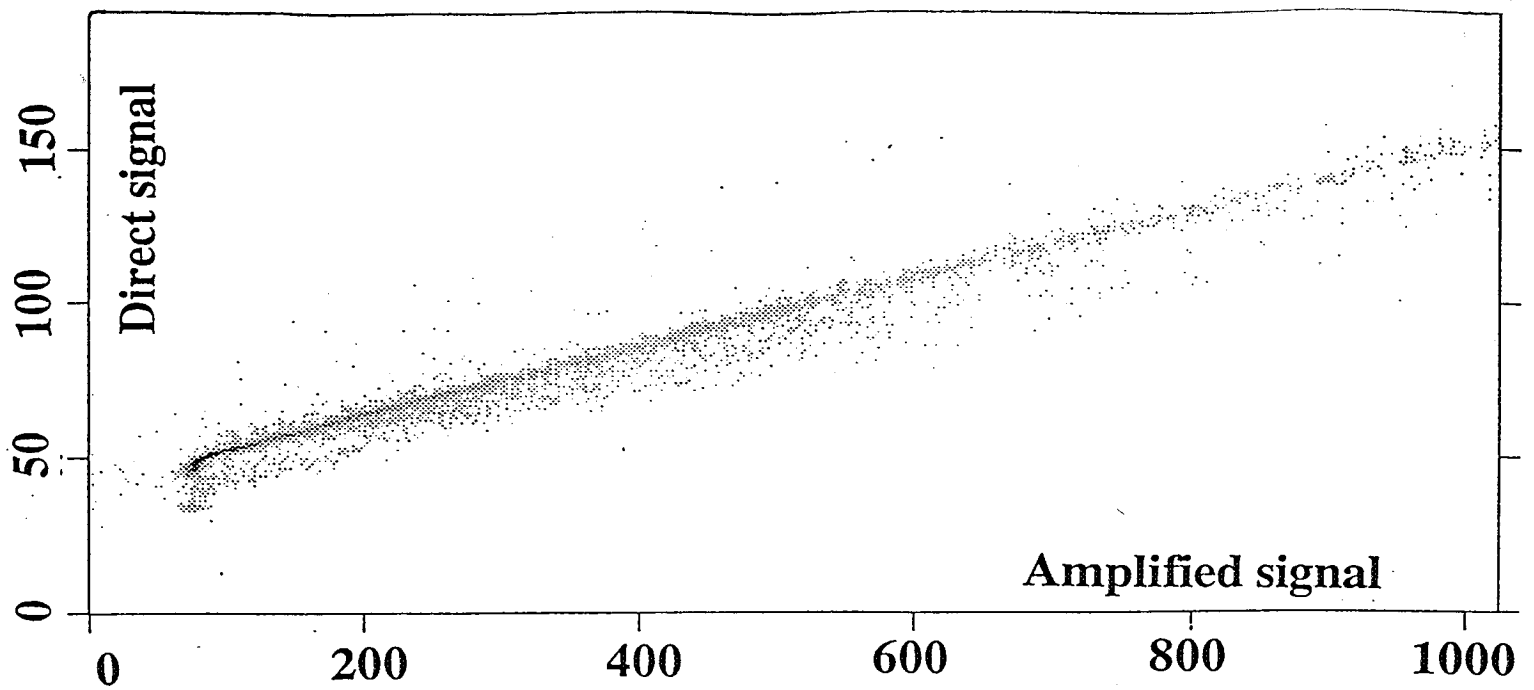Fig 2.1 p The fractional yield of iron events

Fig 2.3 a Amplified signal (abscissa) against the direct signal. Note the faint ghosting, from bit errors, and the non-linear behavior for small amplitudes
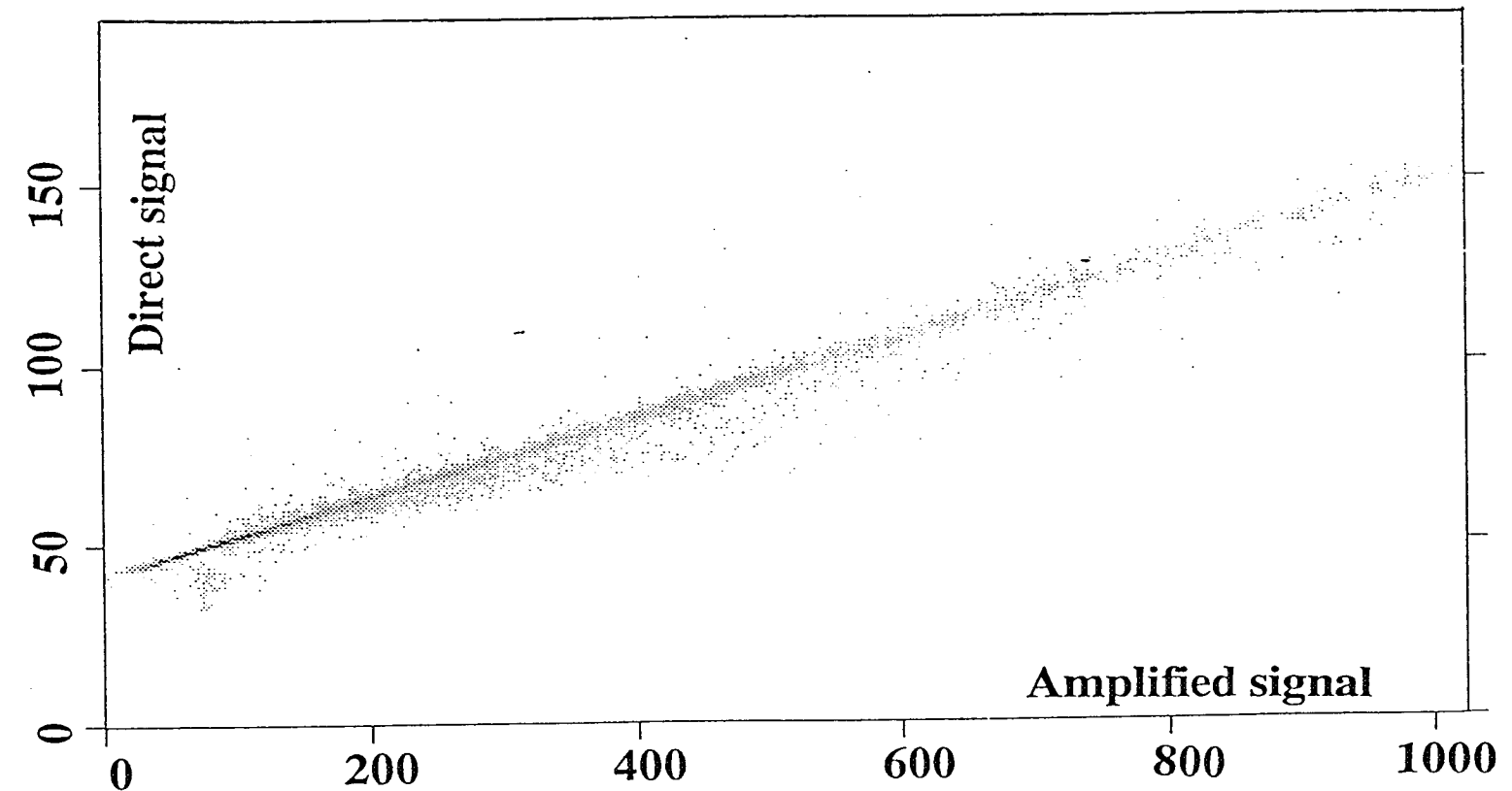

Fig 2.3 b As fig 2.3a, but after application of a linear correction.

in regions A and C, was digitized directly, and after amplification. To calculate the offsets for both the amplified, and directly fed ADCs the quotient:

$$\text{Amplified signal/ (directly fed signal)}$$

$$= (\text{signal*gain+g\_offset})/(\text{signal +offset})$$

g = amplifier gain

g_offset = offset in amplified channel

offset = offset in direct channel

was calculated. The two offsets were adjusted until the calculated quotient spectrum was sharp, and had a centroid equal to the gain of the amplifier.

2.3 Non-linearity & bit errors

To check for non-linearity 2 parameter plots of the amplified signal (abscissa) against direct (ordinate) were produced. A typical spectrum is shown in fig 2.3a. This shows two features: A faint ghost like second gain line which we attribute to occasional bit errors, and which are easily excluded from the analyzed events, and a non-linear response for small signals. The non-linearity is puzzling, and we have not been able to reproduce it in bench tests although we have duplicated, to the best of our knowledge, the flight electronics. It seems the problem originated in the hybrid amplifier invertor combination that processed the signals rather than the commercial ADC. We have applied a systematic correction, by measuring the amplified centroid as a function of the direct, and then applying a linear correction to move this centroid on to the same gain line as the larger signals. This procedure works well as shown in fig 2.3b. Flux simulations using the normalization's from HEAO (ref. 1), are in good agreement with the detected yields, giving confidence that no significant data loss occurred.

2.4 Gain matching

Once the offsets, and non-linearites were corrected the gains were matched by gating on the iron, and silicon signals in B. This was performed iteratively, using the deduced A and C signals to refine B, and repeating. This procedure was checked by taking the ratio of the iron to silicon peaks. This ratio should, if all the gains and offsets are correct, be simply the quotient of the square of the nuclear charges: $26**2 / 14**2 = 3.45$, and this was found to be the case.

2.5 Preliminary analysis

Regions A and C are designed to work as optical cavities. Cerenkov light released in the pilot, which is predominantly in the UV, is wavelength shifted to 425 nm. The light which would normally be trapped in the pilot due to the refractive index mis-match (1.516 for Pilot to ~1 for air) is liberated from the frosted surface, and collected by the eight pairs of tubes which are all equipped with large "fisheyes." The collection efficiency is not uniform. A cosmic ray hitting near the pole will illuminate all the tubes with approximately equal intensity whilst one hitting near the equator will illuminate the close by tube pair at the expense of those on the other side of the hemi-sphere. An added complication arises from events where the cosmic ray hits, or a substantial fraction of delta rays hit, a fish eye; these events must be rejected. Prior to flight the response of region A as a function of

longitude and latitude, was investigated with a UV laser. These measurements have been a useful aid in the analysis process. As a preliminary to developing a correction factor for the latitude, and longitude variation we have developed a technique to map the three dimensional surface of region A in to two dimensions. Attempts to do this based on assigning position relative to the biggest, second biggest, etc. signals were frustrated because the signals are strong functions of position, and the available events in the subset are limited when spread over the large collection area. An approach that requires no *a priori* decision about the impact point was developed by Manuel Grande (a Bristol graduate student who worked on BUGS-4, in Bristol). In the Grande model we construct vectors based on the tube signals as shown if fig 2.4a.

$$Vx = I3 - I7 + (I2 + I4)\cos(45) - (I5 + I8)\cos(45)$$
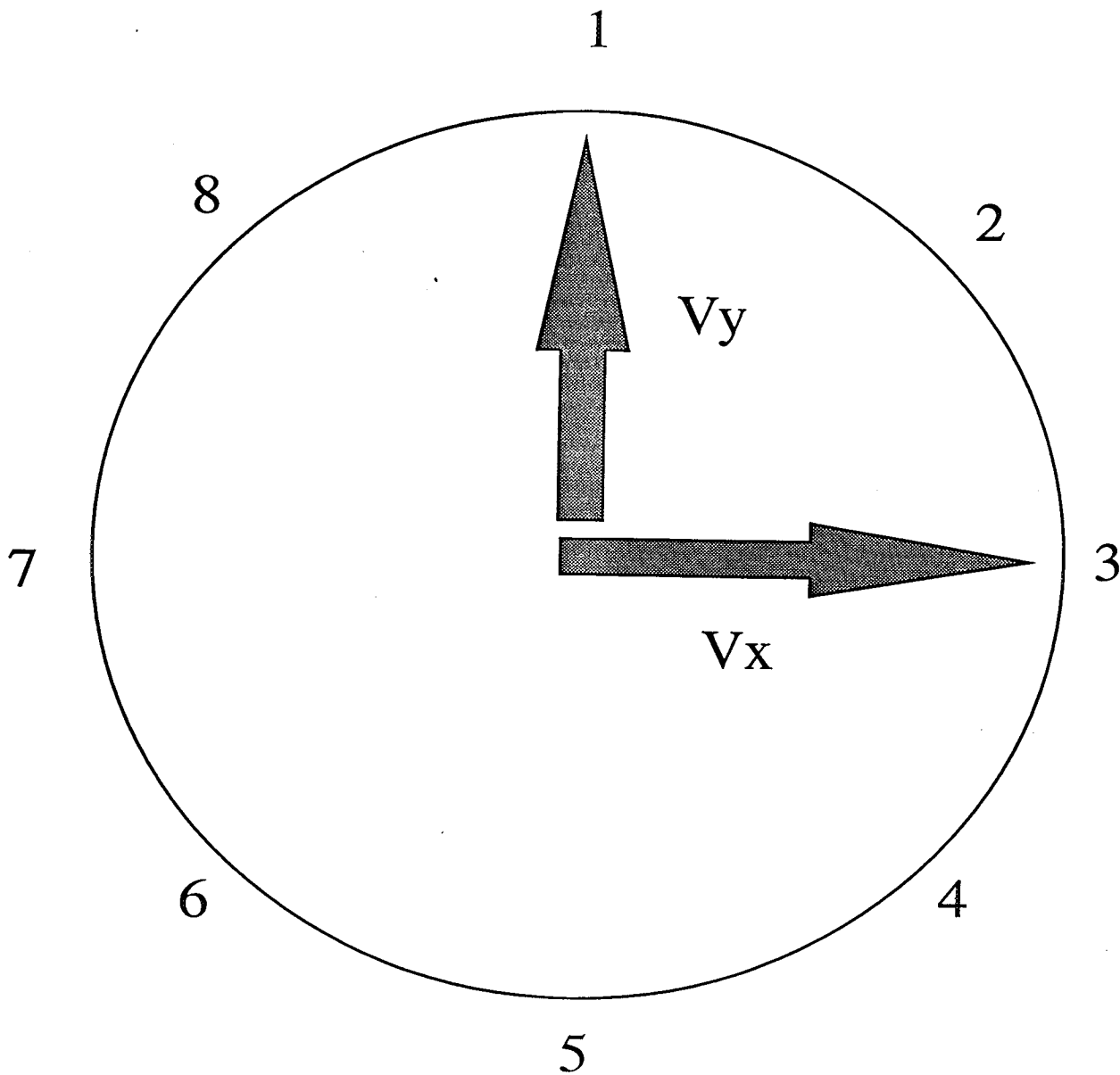
$$Vy = I1 - I5 + (I2 + I8)\cos(45) - (I4 + I6)\cos(45)$$

The two dimensional "longitude" (psi) is then given by arctan(Vy/Vx); the two dimensional "latitude" (theta) is deduced from assuming that Vx, and Vy are projections from the spherical surface:

$$Vx = r \sin(theta)\cos(psi)$$
$$Vy = r \sin(theta)\sin(psi)$$

r is the spherical radius; theta is deduced from these equations. The vectors are normalized by dividing by the total signal, and adjusted so that the maximum length is 100, corresponding to the radius of region B in centimeters. The results of applying this technique to region A are shown in fig 2.4b. The pole of region B was the mounting point for the ceramic probe, and was not covered with pilot. The "hole" is clearly shown in fig 2.4b. In order to investigate the correlation with the path length deduced from region B, gates were placed on polar events in A and C using the Grande approach. These events, as shown in fig 2.4c, correlate well with small impact parameters.

The best method to recover the cosmic ray signal with minimum distortion is still being researched. One approach uses the great circle distance to each tube, whilst simulations in Bristol suggest using the mean of six point five tubes is better than taking the mean of all eight tubes. The analysis is complicated by geomagnetic cut off at Fort Sumner which is 1.18 GeV/a, and once atmospheric slowing is included many cosmic rays will reach BUGS-4 with lower energy. Pilot saturates (95.6%) of maximum (Iron charge 25.5) for energies beyond 4 GeV/a. Hence a large fraction of the events do not saturate the Pilot radiator. Further work will allow a charge spectrum for the unsaturated events to be created by combining the region A and region B signals. The techniques used to refine the signals in region A, are being applied to region C. Once this work is complete the >20 GeV/a events will be extracted. This procedure is complicated, because the freon events are superimposed on the pilot Cerenkov signals. A fully saturated freon Cerenkov event produces a signal that is equal to that from the pilot. However, saturation (95.6%) of maximum does not occur until 110 GeV/a. Flux simulations indicate about one event in 350 will fully saturate the freon Cerenkov. If we consider particles that have an energy greater than 37.3 GeV/a producing a signal that is 70% of saturation (Iron charge 21.75), we expect, from flux simulations, only 1.4% of the events will meet this criterion.

$$Vx=I3-I7+(I2+I4)\cos(45)-(I6+I8)\cos(45)$$

$$Vy=I1-I5+(I2+I8)\cos(45)-(I4+I6)\cos(45)$$

Fig 2.4a The Grande geometry

**Raw impact spectrum from B
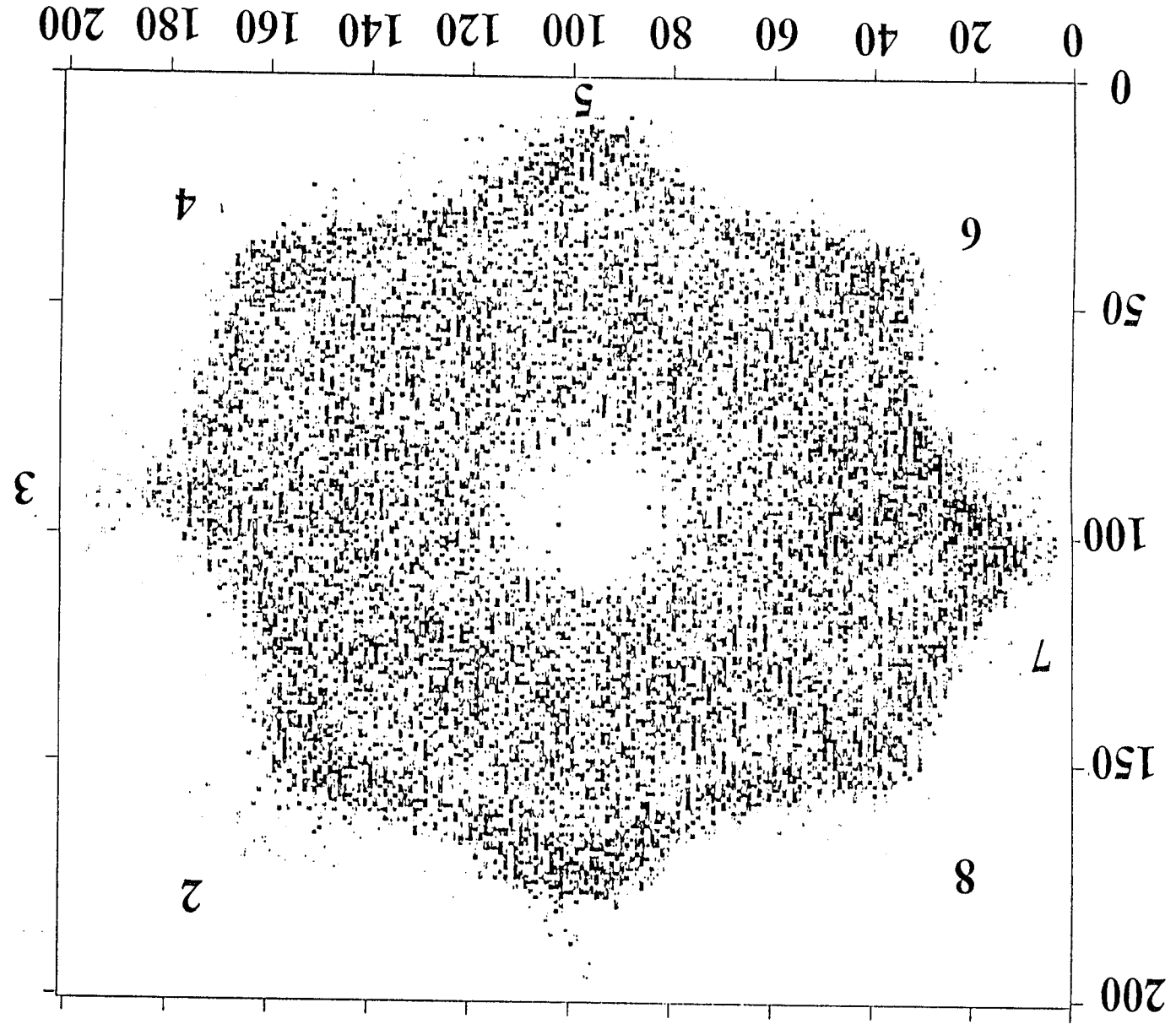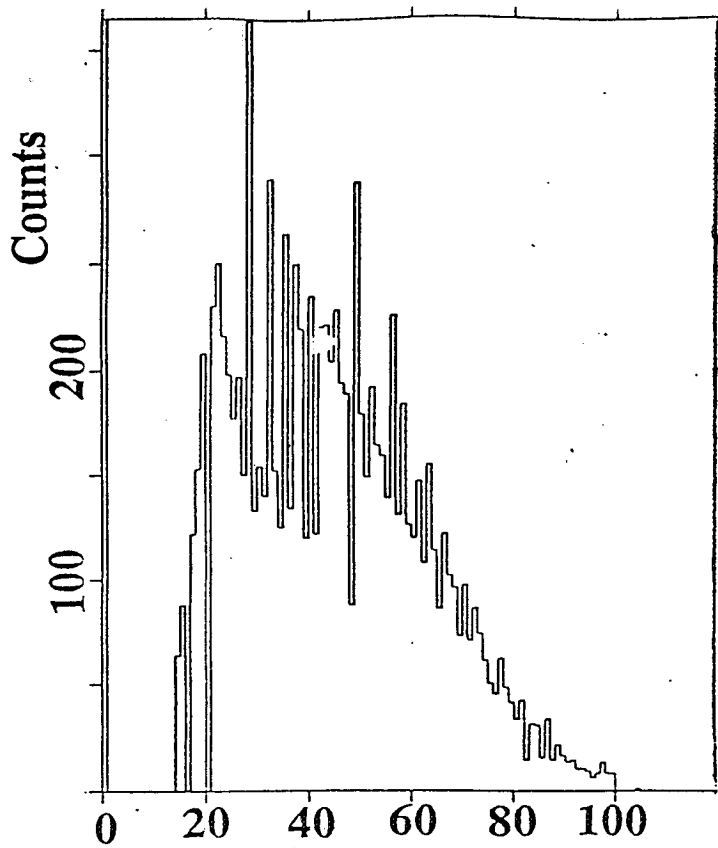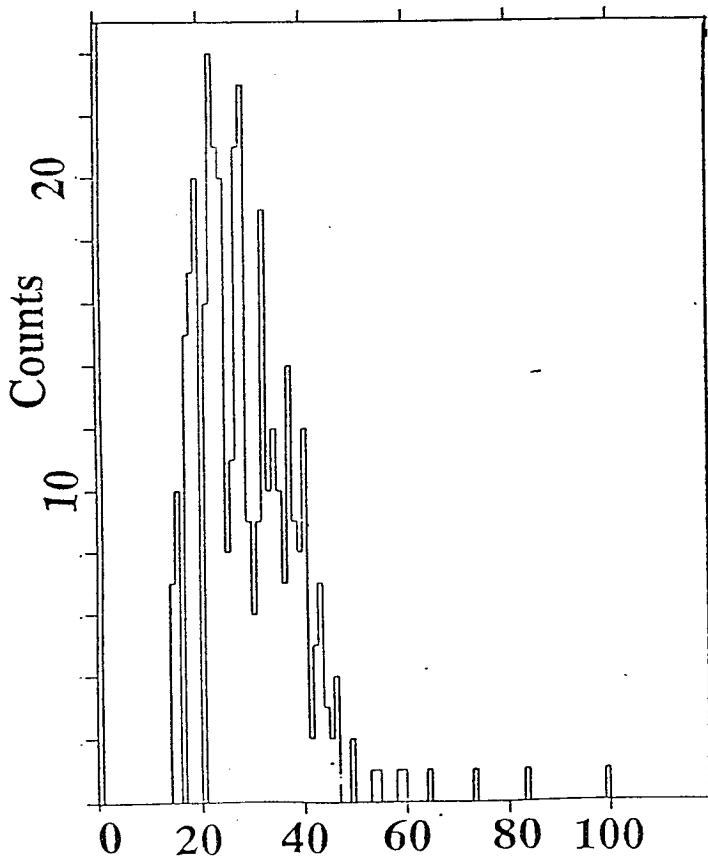The edge of the coincidence
acceptance is at 100.**

**Impact spectrum gated on polar
events in regions A & C**

Fig 2.4 c Correlation between the impact parameter,
measured in B, and polar events in A, and C deduced
from the Grande model.

Hence, it is essential to understand the response of region C particularly with respect to direct fish eye hits or delta rays reaching the fish eyes. Such events can be identified by the signal distribution in C, and also from their expected location in two parameter plots of C against B. This work is still embryonic, because region B has still to be studied in detail as we now discuss.

3.0 Region B: The spherical drift chamber

Introduction:

BUGS-4 achieved its large aperture factor (4.5 m**2str), but low mass by employing a large spherical drift chamber that provides both energy measurement, and impact parameter determination. The flight of this large spherical drift chamber was a notable first for the sub-orbital program. During this report period we have primarily concentrated on regions A and C since these will provide the charge determining elements, that will allow us to track gain variations in the full data set, once the systematic corrections are deduced from the sub-set of 30,000 events. To aid this work we have refined the impact calculation to recover events that were contaminated with bit errors. Although our study of region B during this report period has been small it will become the focus of future work.

3.1 Bit errors in region B

A number of drift events in region B show bit errors where the drift signal is offset by 64 as shown in fig 3.1a. Algorithms have been developed to detect, and correct such events. Fig 3.1b is the same as fig 3.1a, but after processing with the correction algorithms.

4.0 Summary & conclusion

During the report period significant progress has been made toward correcting several systematic errors in a small subset of the data. Techniques have been developed to check the time stability, deduce the flight gains, and ADC pedestals. Region A and C have been mapped in to a two parameter latitude, and longitude space, which correlates with the impact parameter deduced from region B. At present region B has not been studied in detail, but techniques have been developed to correct bit errors in the drift signal. Future work will be directed towards extracting an optimum charge spectrum from region A, by correcting for the non-linear light collection, and using the scintillation signal from region B to process the majority of the events which, due to the geomagnetic cutoff at Fort Sumner, do not saturate the Cerenkov radiators. To aid with this task we will investigate the relation between the primary, and gas proportional scintillation signals, which should be the best measure of the primary scintillation. At present little work has been done on the Freon gas Cerenkov signal, and no work has been performed on the gas Cerenkov signal in B. Although there are only a few high energy events in the small subset where we have concentrated our attention we hope to extract these events as our understanding increases. The problems encountered have been technological, and not with BUGS-4. We are confident that future analysis will show the design concept is sound, and justifies a rebuild.

Reference

(1) Engelmann J. J., *et al* Astronomy, and Astrophysics **233** 1990 96
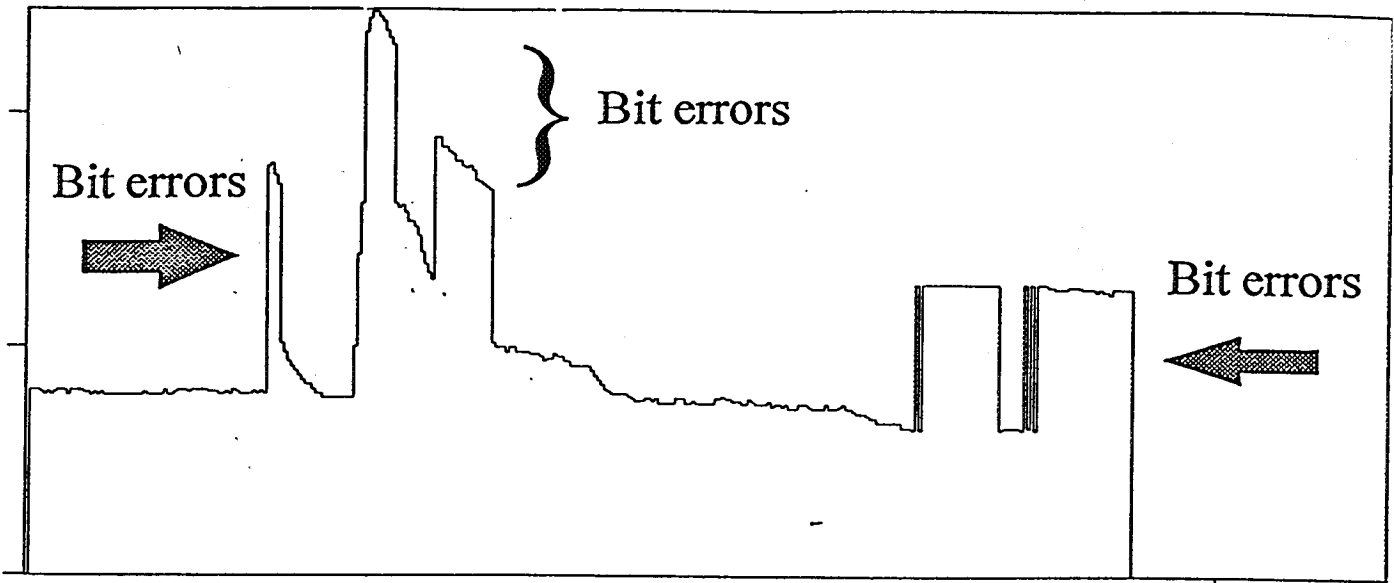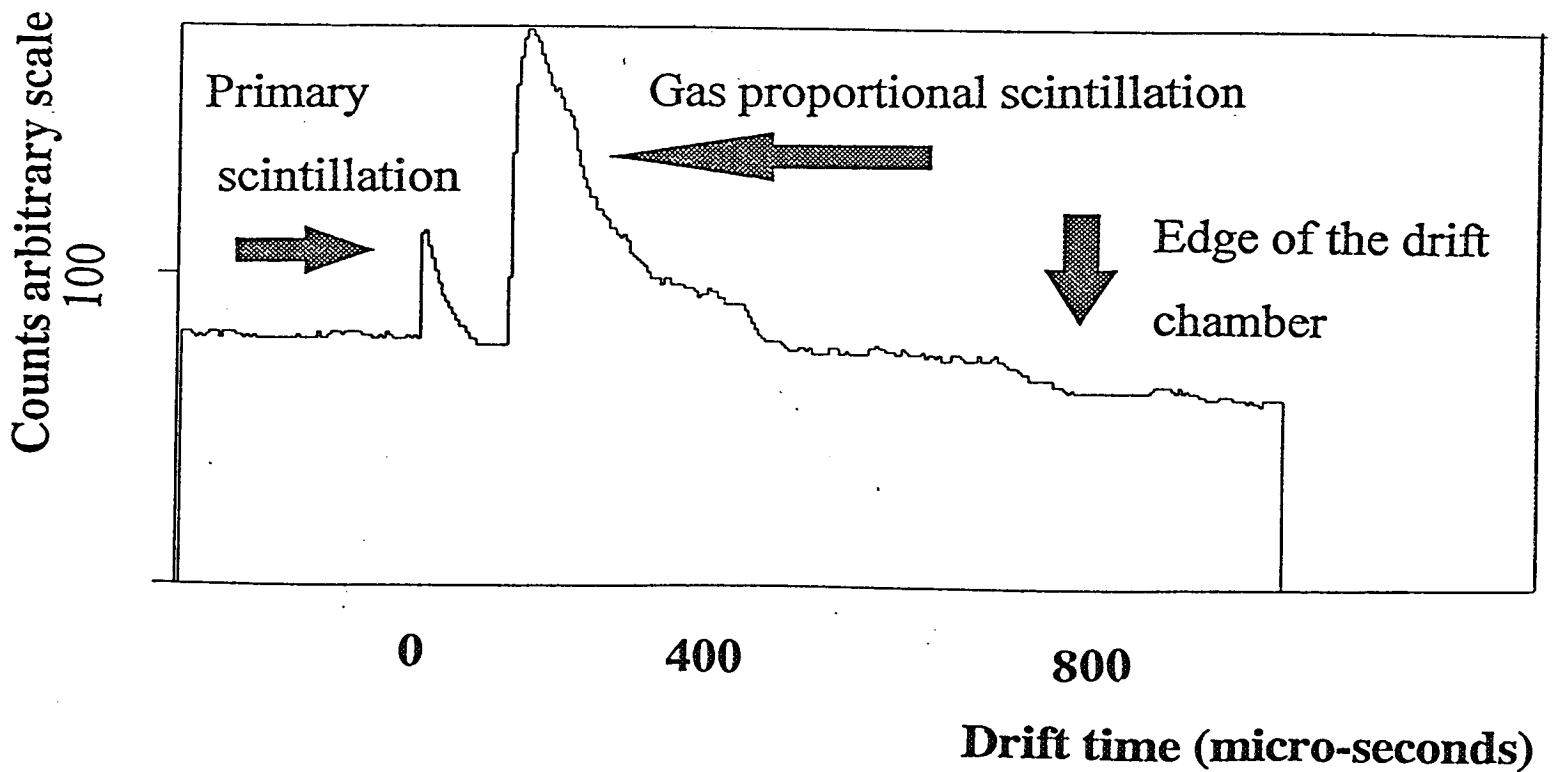
Fig 3.1 a A drift spectrum contaminated by bit errors

Fig 3.1 b As 3.1b, but after application of the correction algortihms